Science of the Total Environment 847 (2022) 157645

Contents lists available at ScienceDirect

Science of the Total Environment

journal homepage: www.elsevier.com/locate/scitotenv

Differential responses of fungal and bacterial necromass accumulation in soil to nitrogen deposition in relation to deposition rate

Peng Tian [a,b], Xuechao Zhao [b,i], Shengen Liu [c], Qinggui Wang [d], Wei Zhang [e], Peng Guo [f], Bahar S. Razavi [g], Chao Liang [h], Qingkui Wang [a,b,*]

[a] School of Forestry and Landscape Architecture, Anhui Agricultural University, Hefei 230036, China
[b] Huitong Experimental Station of Forest Ecology, CAS Key Laboratory of Forest Ecology and Management, Institute of Applied Ecology, Shenyang 110016, China
[c] College of Biological and Pharmaceutical Sciences, China Three Gorges University, Yichang 443002, China
[d] School of Life Sciences, Qufu Normal University, Qufu 273165, China
[e] South China Botanical Garden, Chinese Academy of Sciences, Guangzhou 510650, China
[f] Department of Chemical and Environmental Engineering, Hebei College of Industry and Technology, Shijiazhuang 050091, China
[g] Dept. Soil and Plant Microbiome, Institute of Phytopathology, Christian-Albrechts-University of Kiel, 24118 Kiel, Germany
[h] Key Laboratory of Forest Ecology and Management, Institute of Applied Ecology, Chinese Academy of Sciences, Shenyang 110016, China
[i] University of Chinese Academy of Sciences, Beijing 100049, China

HIGHLIGHTS

- Low N deposition damaged the accumulation of bacterial necromass.
- High N deposition benefitted fungal necromass accumulation.
- The accumulation of microbial necromass was primarily governed by soil properties.
- N deposition didn't change the latitudinal distribution of microbial necromass accumulation.

GRAPHICAL ABSTRACT

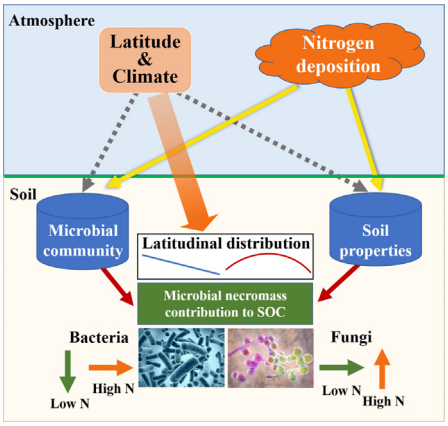

ARTICLE INFO

Editor: Zhaozhong Feng

Keywords:
Microbial necromass
Amino sugars
Soil organic carbon sequestration
Nitrogen deposition
Geographical distribution
Forest ecosystem

ABSTRACT

Influenced by nitrogen (N) deposition, changes in soil organic carbon (SOC) sequestration in terrestrial ecosystems could provide strong feedback to climate change. Mounting evidence showed that microbial necromass contributes substantially to SOC sequestration; however, how N deposition influences microbial necromass accumulation in soils remains elusive. We investigated the impacts of N deposition on soil microbial necromass, assessed by amino sugars, at seven forest sites along a north-south transect in eastern China. We found that the responses of fungal and bacterial necromass accumulation to N deposition depended on the deposition rate, with high N deposition (>50 kg N ha^{-1} yr^{-1}) stimulating fungal necromass accumulation from 29.1 % to 35.2 %, while low N deposition damaging the accumulation of bacterial necromass in soil by 12.1 %. On the whole, N deposition benefitted the dominance of fungal over bacterial necromass, with their ratio being significantly greater at high-N level. The accumulation of microbial necromass was primarily governed by soil properties, including nutrients stoichiometry, clay content and

* Corresponding author at: School of Forestry and Landscape Architecture, Anhui Agricultural University, Hefei 230036 China.
E-mail address: wqkui@163.com (Q. Wang).

http://dx.doi.org/10.1016/j.scitotenv.2022.157645
Received 25 May 2022; Received in revised form 13 July 2022; Accepted 22 July 2022
Available online 28 July 2022

pH, while the composition of microbial necromass was conjointly affected by soil properties and microbial community structure. The latitudinal distribution of microbial necromass contributions to SOC pool was not altered by N deposition, and was firmly controlled by the climatic and edaphic factors. Collectively, our results reveal the impacts of N deposition on microbial necromass accumulation in soil and the geographical pattern across forest ecosystems in eastern China, providing implications for our accurate predictions of global change impacts on SOC sequestration.

1. Introduction

Soil organic carbon (SOC) is the largest active C pool in terrestrial ecosystems, storing approximately 1500 Pg C in the upper 100 cm layer (Lal, 2008), thus minor changes in SOC sequestration could result in strong feedback to climate change (Schmidt et al., 2011; Lehmann and Kleber, 2015). In recent decades, mounting evidence had suggested that microbial necromass plays a more important role in SOC sequestration than traditionally considered (Liang and Balser, 2011; Miltner et al., 2012; Ludwig et al., 2015; Liang et al., 2017). Microbial necromass is produced during microbial biomass turnover via iterative processes that involve cell generation, population growth, death, and decay, serving as a time-integrated indicator (Liang and Balser, 2011; Cotrufo et al., 2015; Ludwig et al., 2015; Liang et al., 2017; Ni et al., 2021). In contrast to the small proportion of microbial biomass in SOC (< 4 %), microbial necromass accounts for potentially more than half of the SOC pool (Liang and Balser, 2011; Miltner et al., 2012; Liang et al., 2017; Ni et al., 2020a). Nitrogen (N) deposition, a global change-related factor, has been widely demonstrated to potentially enhance SOC sequestration in terrestrial ecosystems through stimulating soil aggregation and acidification (Lu et al., 2021a, 2021b). At individual sites, N deposition could mediate microbial necromass accumulation in soil through their influence on microbial processes (Griepentrog et al., 2014; Zhang et al., 2016; Fan et al., 2020; Ma et al., 2020). However, how increased N deposition influences the accumulation of microbial necromass in SOC pool and its geographical pattern at large scales remain elusive.

Due to the tight coupling of C and N cycles in terrestrial ecosystems, N deposition or fertilization can substantially influence microbial necromass accumulation by altering the microbial growth and biomass turnover (Wang et al., 2017; Widdig et al., 2020). For example, as affected by N deposition, the microbial necromass contents and their proportions to SOC in surface soil layers were found to increase significantly (Griepentrog et al., 2014; Chen et al., 2020a; Fan et al., 2020; Ni et al., 2020a). In contrast, inhibitory effects of N deposition on the contribution of microbial necromass to SOC were also detected, especially under high N deposition rates (Liang and Balser, 2012; Zhang et al., 2016). These observations were not consistent partly because of the variations in N deposition rate in combination with edaphic and climatic characteristics among investigations. Additionally, compared with bacteria, fungi have been shown to be more sensitive to changes in soil N availability and thus respond more rapidly to external N input (Gutknecht et al., 2012; Wang et al., 2017; Widdig et al., 2020). Empirically, N deposition exerts a greater influence on the accumulation of fungal necromass than bacterial necromass, mostly enhancing the fungal necromass accumulation via enhancing physical protection from decomposition as well as stimulating fungal necromass formation (Griepentrog et al., 2014; Luo et al., 2020). To date, however, knowledge of the responses of bacterial and fungal necromass to various levels of N deposition is limited, constraining an in-depth understanding of the coupling of C and N cycles in terrestrial ecosystems.

Until now, little information has been available on whether increased N deposition alters the geographical pattern of microbial necromass accumulation in forest SOC pool at a large scale. Generally, the higher temperature in subtropical and tropical forests is more suitable for microbial turnover than in temperate forests. In addition, soil nutrients availability varies greatly across forest biomes from temperate to tropical zones (Du et al., 2020), which affects microorganism turnover and subsequent necromass accumulation at the macroscale (Geyer et al., 2016; Jones et al., 2018). However, this rule can be restricted by the coupled lower soil pH in warmer zones, which restricts enzyme diffusion and limits microbial activity, resulting in less microbial necromass C accumulation (Chi et al., 2019; Wilpiszeski et al., 2019). Therefore, the geographical pattern of the contributions of microbial necromass to SOC was affected by climate and soil physicochemical properties conjointly, probably showing a nonlinear geographical pattern (Chen et al., 2020a; Ni et al., 2020a). However, whether the geographical pattern of microbial necromass accumulation was susceptible to changes in soil physicochemical and microbial traits following increased N deposition, or firmly governed by climatic factors remains unclear (Ma et al., 2020; Widdig et al., 2020).

Here, along the latitudinal gradient in eastern China, we collected soils samples from seven forest ecosystems where simulated N deposition experiments were conducted. Amino sugars, widely accepted biomarkers, were used to trace microbial necromass in soils (Ma et al., 2018; Liang et al., 2019). In this study, our aims were 1) to explore how N deposition at different levels influences bacterial and fungal necromass to SOC accumulation; and 2) to reveal whether the latitudinal distribution of microbial necromass to SOC accumulation is affected by N deposition in forest ecosystems along a north-south transect. On the basis of the stronger sensitivity of fungi compared with bacteria to N enrichment, N deposition was expected to induce different impacts on the accumulations of fungal and bacterial necromass. We hypothesized a strong enhancement of fungal necromass by N deposition in particular. Furthermore, previous studies have demonstrated that the spatial variations in microbial processes and functions at a large scale are mostly affected by climatic factors, with thermal condition primarily controlling the decomposition and accumulation of SOC in forest ecosystems along the north-south transect (Luo et al., 2020; Ma et al., 2020; Ni et al., 2020b). Therefore, it was hypothesized that the latitudinal distribution of microbial necromass accumulation in forest ecosystems might be less susceptible to N-induced changes in soil properties.

2. Materials and methods

2.1. Study sites

In this study, soils were collected from seven forest sites across China with a wide array of climate and soil environment conditions: Heshan (HS), Qianyanzhou (QYZ), Huitong (HT), Jigongshan (JGS), Hebei (HB), Xiaoxinganling (XX), and Daxinganling (DX). These sites have distinct soil properties and climate conditions with a mean annual temperature (MAT) range of −2.4 °C to 21.7 °C and mean annual precipitation (MAP) range of 350 mm to 1700 mm (Table 1). Long-term simulated N deposition experiments have been established for at least 5 years. Nitrogen fertilizer was applied as ammonium nitrate (NH_4NO_3) and was dissolved in water and sprayed. Due to these N deposition experiments were established by different research teams, the frequency of fertilizer addition varies from once a year to once a month. The control plot received the same volume of water as N-treated plots. The experiments generally included three treatments in triplicates or quadruplicate: control (no fertilization, CT), low N deposition ($\leq$50 kg N ha^{-1} yr^{-1}) and high N deposition (>50 kg N ha^{-1} yr^{-1}). Detailed information about the long-term simulated N deposition experiment at each site is provided in Table 1.

2.2. Soil collection and chemical analysis

Soil samples were collected from seven forest sites in August 2017. In each plot, after removing litter layer, 8–10 soil cores were randomly collected from the top 10 cm of mineral soil using a metal corer with a 5 cm diameter and then mixed into a composite sample. In total, 134 composite

Table 1
Geographical location and environmental conditions of the sites and the corresponding long-term simulated N deposition experiment.

Site	Latitude (N)	Longitude (E)	MAT (°C)	MAP (mm)	Soil type	Vegetation type	Duration (yr)	Frequency (n yr^{-1})	N level (kg N ha^{-1} yr^{-1})
HS	22°40′	112°54′	21.7	1700	Laterite	Broad-leaved evergreens	9	12	50/100
QYZ	26°41′	115°04′	17.9	1360	Red earth	Broad-leaved evergreens	9	1	50/100
HT	27°05′	109°30′	16.5	1200	Ultisol	Chinese fir plantation	7	1	200
JGS	31°52′	114°5′	15.3	1108	Yellow brown earth	Deciduous broad-leaved forest	5	12	25/50
HB	37°54′	114°21′	13.3	520	Cinnamon soil	Deciduous broad-leaved forest	7	4	72
XX	48°7′	129°11′	−0.5	700	Dark brown soil	Conifer broadleaf mixed forest	9	6	50/100
DX	51°7′	125°9′	−2.4	489	Grey forest soil	Coniferous forest	7	6	25/50

MAT and MAP denote the mean annual temperature and mean annual precipitation, respectively.

soil samples were built. All soil samples were transported with a low-temperature incubator (~4 °C) to the laboratory within 24 h after collection and then passed through a 2 mm mesh to eliminate residual organic matter (i.e., decomposed leave litter and roots). The soils used for chemical and microbial property determination were air-dried and freeze-dried, respectively.

Soil organic C and total N were measured using a C/N analyzer (Elementar, Germany). Soil total phosphorus (P) was measured colorimetrically. Soil mineral N (sum of ammonium and nitrate N) was extracted using 2 M KCl solution and determined using colorimetry (Lu, 2000). Available P was analyzed colorimetrically through the molybdate blue method after the soil was extracted with 1 M NH_4F solution. Soil pH was determined using a pH meter in a 1:2.5 (weight: volume) mixture of soil and deionized H_2O after shaking for 30 min. The soil texture (sand, silt, and clay contents) was analyzed according to the pipette method (Lu, 2000).

2.3. Soil microbial community structure as assessed by PLFA

Phospholipid fatty acid (PLFA) analysis was conducted to reveal soil microbial community composition (White and Ringelberg, 1998). Briefly, phospholipids were extracted from 3 g of frozen dry soil using the chloroform–methanol extraction with a 0.05 M phosphate buffer and then fractionated and quantified. The resultant fatty acid methyl esters were identified using a gas chromatograph (GC; 6890A, Agilent, USA) equipped with the MIDI Sherlock Microbial Identification System (MIDI, Inc., Newark, DE, USA). Total bacterial content was derived as the sum of i15:0, a15:0, 15:0, i16:0, 16:1ω7c, 16:1ω9c, 16:0, a17:0, i17:0, cy17:0, 17:0, 18:0, cy19:0, and 20:0 PLFAs. Gram-positive bacteria were identified by the terminal and mid-chain branched fatty acids (i15:0, a15:0, i16:0, i17:0, a17:0), and cyclopropyl saturated and monosaturated fatty acids (16:1ω7c, cy-17:0, 18:1ω7c, 8cy-19:0) were considered indicative of gram-negative bacteria (Rinnan and Bååth, 2009). The fatty acids 18:1ω9(c,t) and 18:2ω9,12c were used as markers for fungi (Kaiser et al., 2010).

2.4. Soil microbial necromass as assessed by amino sugars

Soil amino sugars were extracted according to Zhang and Amelung (1996). In brief, weighed soil samples were hydrolyzed with 6 M HCl for 8 h, and the solution was later filtered, pH adjusted (6.6–6.8), centrifuged, and freeze-dried. Next, the freeze-dried supernatants received methanol and were subsequently centrifuged to extract amino sugars. The purified amino sugars were reacted with hydroxylamine hydrochloride and 4-(dimethylamino) pyridine (in a first step) and acetic anhydride (in a second step) at 75–80 °C to produce volatile aldononitrile acetates. The amino sugar derivatives were separated in a GC (6890A, Agilent, USA) equipped with an HP-5 column (30 m × 0.25 mm × 0.25 μm). Myoinositol was added prior to purification as internal standard, and *N*-methylglucamine were added before derivatization as the standards to measure the recovery of amino sugars. The ratio of glucosamine (GluN) to muramic acid (MurN) was used to evaluate the relative retention of fungal and bacterial necromass. Bacterial and fungal necromass were calculated from the concentrations of MurN and GluN, respectively, based on the empirical conversion factors.

$$\text{Bacterial necromass C (mg/g soil)} = \text{MurN (mg/g soil)} \times 45 \quad (1)$$

where 45 is the conversion factor from MurN to bacterial necromass C (Appuhn and Joergensen, 2006).

Fungal necromass C was calculated by subtracting bacterial GluN from total GluN as an index for fungal necromass, assuming that MurN and GluN occur at a 1:2 M ratio in bacterial cells:

$$\text{Fungal necromass C(mg/g soil)} = (\text{GluN(mg/g soil)}/179.17\text{–}2 \times \text{MurN(mg/g soil)}/251.23) \times 179.2 \times 9 \quad (2)$$

where 179.2 is the molecular weight of GluN and 9 is the conversion value of fungal glucosamine to fungal C (Appuhn and Joergensen, 2006). The total microbial necromass C is the sum of fungal and bacterial necromass C.

2.5. Statistical analyses

Before analysis, the Kolmogorov–Smirnov test was performed to determine whether all data were normally distributed. If not, $\log_{10}$-transformation was conducted to meet data normality assumptions. To analyze the effects of N deposition on PLFAs, microbial necromass and their contributions to SOC, linear mixed-effects models were performed with site as random factor. Pairwise comparisons of means were tested by the least significant difference multiple-comparison post hoc test. Pearson's correlation analysis was conducted to evaluate the relationships between the contribution of microbial necromass to SOC and soil physicochemical and microbial properties. Further, variance partitioning and partial least squares path model (PLS-PM) were performed to unravel out the importance of variables in determining the contribution of microbial necromass to SOC pool and the ratio of fungal to bacterial necromass. Variation partitioning analysis based on “packfor” and “vegan” packages was performed to assess the relative importance of two groups: soil physicochemical properties and microbial characteristics. The “forward.sel” function was used to avoid redundancy and multicollinearity in variation partitioning analysis. PLS-PM is a data analysis approach for variables that can be summarized by using latent variables, and the fact that linear relationships exist between latent variables (Sanchez, 2013). Two latent variables, i.e., soil properties and microbial characteristics were included in our PLS-PM. Given that soil samples were collected from different sites, it is important to include “site” as random factor in PLS-PM in order to reveal the unmixed role of variables. The statistical analyses were conducted using SPSS and R 4.0.2 (R Development Core Team, 2020) with packages “nlme”, “lme4”, “vegan”, and “plspm”.

3. Results

3.1. Responses of microbial necromass accumulation to N deposition

High-N deposition led to a significant increase in total microbial necromass ($p < 0.05$), which stemmed from the 31.2 % higher fungal

necromass in High-N soils relative to the control soils ($p < 0.05$), whereas bacterial necromass in the soils was not affected by N deposition (Fig. 1a). Low-N deposition decreased the contributions of total microbial necromass to SOC pool by 12.1 % ($p < 0.05$), with bacterial proportions contributing to the inhibition effect primarily ($p < 0.05$; Fig. 1b). In contrast, High-N deposition increased the fungal necromass contribution to SOC pool from 29.1 % to 35.2 % ($p < 0.05$). On the whole, larger contents and contributions of fungal necromass to SOC pool were detected compared with the bacterial necromass. N deposition further increased the ratio of fungal to bacterial necromass, with this effect being significant in High-N treatments ($p < 0.05$; Fig. 1c).

3.2. Regulators of the microbial necromass response to N deposition

The contribution of microbial necromass to SOC pool were closely associated with soil properties and microbial community structure across N deposition treatments (Fig. 2). Remarkably, soil properties have consistently larger contribution in shaping the variation in microbial necromass accumulation across N-amended and control soils (Fig. 3a-c). In contrast, microbial community structure had substantial importance in shaping the variation in ratio of fungal to bacterial necromass in SOC across N-amended and control soils, despite still weaker than soil properties (Fig. 3d). Specifically, C/P ratio and total P were determined to impact the response of bacterial necromass accumulation to N deposition, whereas C/N ratio and total N mediated fungal necromass accumulation (Fig. 3e and f). Two stoichiometric ratios, soil C/N and C/P ratio, primarily influenced the response of total microbial necromass accumulation to N deposition (Fig. 3g). In addition, soil pH and clay contents exerted great influence on the effect of N deposition on the contributions of microbial necromass to SOC pool. In the case of fungal to bacterial necromass, microbial community structure was found to exert substantial effects on the response to N deposition, accompanying with soil properties (Fig. 3h).

A closer examination showed that both low- and high-N deposition decreased the contribution of bacterial necromass to SOC mostly in soils with lower clay contents and those with less acidity (Fig. 4a and b). High-N deposition increased the contributions of fungal necromass to SOC pool in soils with less clay content and in those that were less acidic (Fig. 4c and d). In contrast, the association between fungal necromass accumulation and pH value was not strongly affected by low-N deposition.

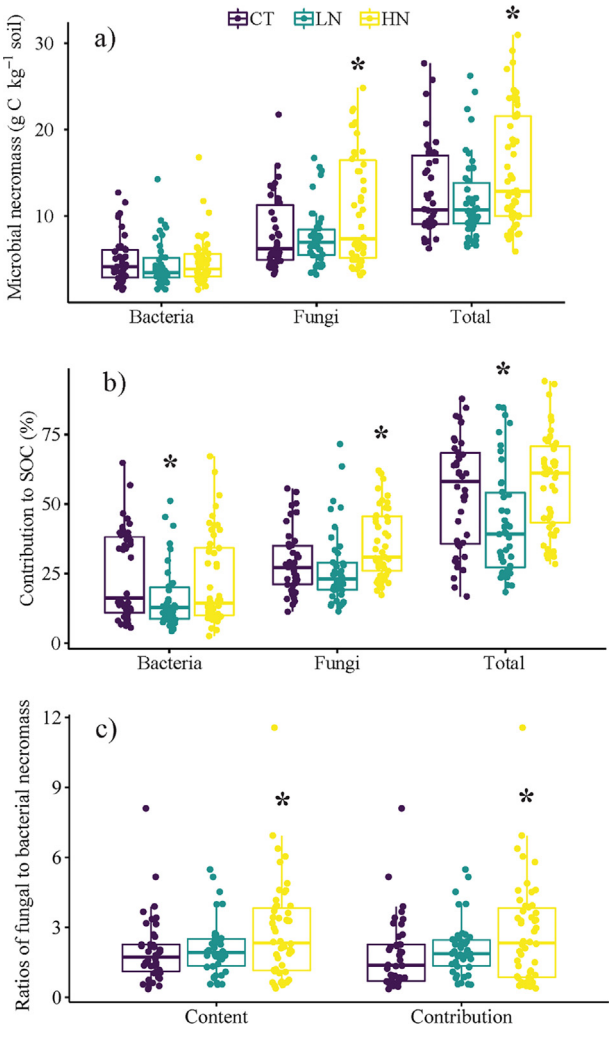

Fig. 1. Soil bacterial, fungal and total microbial necromass (a) and their contributions to SOC pool (b) and the ratios of bacterial to fungal necromass contents and contribution (c) in forest ecosystems under long-term N deposition. The asterisks denote significant differences from the control treatment at $p < 0.05$. CT, LN, and HN indicate control (no fertilization, n = 38), low N deposition (≤50 kg N ha^{-1} yr^{-1}, n = 66) and high N deposition (>50 kg N ha^{-1} yr^{-1}, n = 30) treatments, respectively.

3.3. N-induced changes in latitude dependence of microbial necromass accumulation

The contribution of fungal and total microbial necromass to SOC pool exhibited a hump-shaped pattern with increasing latitude and peaked at approximately 35°N (Fig. 5b and c). This apparent pattern primarily stemmed from the hump-shaped distribution of fungal and total microbial necromass concentrations as the latitude increased (Fig. S1). The maximal contributions of fungal and total microbial necromass to SOC pool were estimated to be 40.9 % and 61.5 %, respectively. In contrast, a linear fit was better than polynomial fit for the bacterial necromass contribution to SOC pool, which decreased with latitude (Fig. 5a). The latitudinal patterns of microbial necromass contribution to SOC pool were not changed by N deposition, with the standardized N-induced changes in microbial necromass contribution to SOC pool showing little difference across studied sites (Fig. S2).

4. Discussion

4.1. Effects of N deposition on soil microbial necromass accumulation

The contribution of microbial necromass to SOC pool in this study fell within the ranges of previous observations at the equilibrium stage, ranging from 47 % to 80 % depending on the plant litter quality and the amount of remaining plant-derived biomass (Liang et al., 2017; Kästner and Miltner, 2018). Numerous studies have clarified that part of SOC is directly generated from plant residues via ex vivo modification pathways, and the rest is derived from microbial necromass (Liang et al., 2017). Given the stable total microbial necromass contents in the low-N treatment and greater contents in the high-N treatment (Fig. 1a), notably, the decreased contributions of microbial necromass to SOC pool in the low-N treatment and stable contributions in the high-N treatment (Fig. 1b) indicated that SOC storage was enhanced by N deposition. Our results of increased SOC content under N deposition also supported this explanation firmly (Fig. S3). Previous studies have pointed that N enrichment benefits the accumulation of plant-derived C via inhibiting the decomposition of litter (Janssens et al., 2010; Chen et al., 2020b; Eastman et al., 2022). Furthermore, an general increase in the accumulation of plant-derived C with N addition could also be due to increased aboveground biomass and thus the production of litter (Thomas et al., 2010; Schulte-Uebbing and de Vries, 2018).

Different responses to N deposition were detected between the contributions of bacterial and fungal necromass to SOC pool (Fig. 1b), demonstrating the variations in bacterial and fungal processing under N enrichment (Wang et al., 2017; Widdig et al., 2020). On the whole, N deposition benefits the accumulation of fungal-derived C at the expense of bacterial necromass in forest ecosystems, verifying our hypothesis and previous site-specific observations (e.g., Griepentrog et al., 2014; Fan et al., 2020).

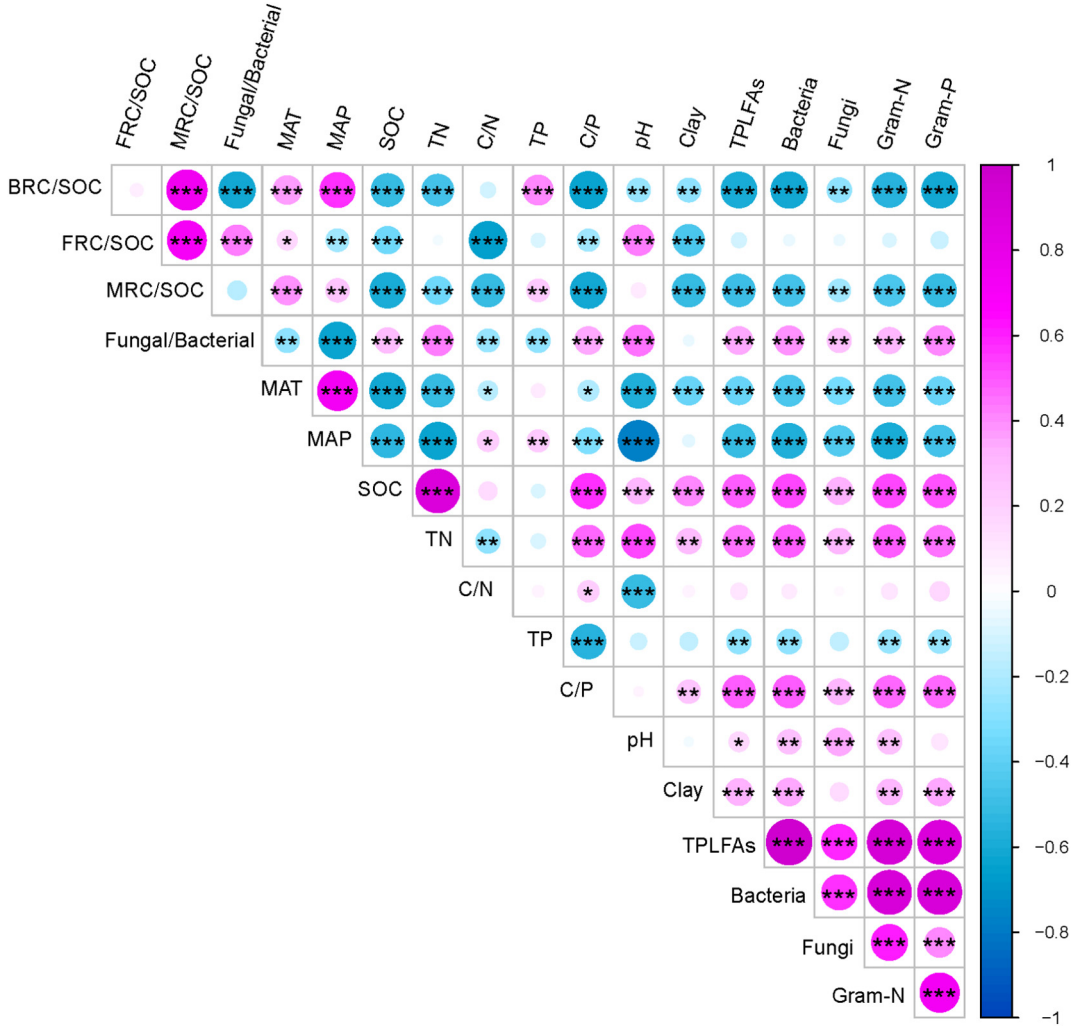

Fig. 2. Pearson's correlation coefficient matrix of the contributions of microbial necromass to SOC and the climatic, edaphic and microbial variables is displayed via a colour gradient. BR/SOC, FR/SOC, and MR/SOC denote the contributions of bacterial, fungal, and total microbial necromass to SOC pool, respectively; TPLFAs denote the total PLFA biomass. AP indicates available phosphorus (P). The asterisk denotes statistical significance: *, $p < 0.05$; **, $p < 0.01$; and ***, $p < 0.001$.

Soil nutrients were suggested to impact the N-induced changes in the accumulation of microbial necromass to SOC (Griepentrog et al., 2014; Ma et al., 2018). Specifically, stoichiometry of soil P and N primarily govern the accumulation of soil bacterial and fungal necromass to SOC in our study, respectively (Fig. 3). Generally, deficiency in soil P availability would lead to increased abundance of EMF and fungi that have high P acquisition ability, ultimately resulting in the decreased contribution of bacterial necromass to SOC accumulation (Fan et al., 2020). As a result, the variations in soil P availability among N deposition treatments or among forest sites with distinct parent materials correlated positively with bacterial necromass contribution (Fig. 3). While the increase in fungal necromass contribution to SOC under high N deposition was likely due to the stimulated microbial derived SOC formation, as indicated by the larger amount of fungal biomass (Fig. S4). Furthermore, decreased decomposition rate of necromass might also attribute to this phenomenon (Griepentrog et al., 2014; Luo et al., 2020). Previous studies have shown that the decomposition of microbial necromass is strongly correlated with soil C/N, which is attributed to the variation in microbial C use efficiency (CUE) (Geyer et al., 2016; Jones et al., 2018). A low C/N ratio in the substrate benefits microbial necromass accumulation by increasing microbial CUE (Cyle et al., 2016; Ni et al., 2020a, 2020b). This suggestion coincides well with our results that the accumulation of fungal necromass was stimulated in soils that received high N deposition (Fig. 1b), where fungal CUE might be stimulated due to the high sensitivity of fungi to changes in soil stoichiometry (Luo et al., 2020; Widdig et al., 2020). Given the role of soil C/N in mediating fungal necromass decomposition (Fan et al., 2020; Luo et al., 2020), fungal necromass more easily accumulates rather than decays under increased N deposition, benefitting the contribution of fungal necromass to SOC pool.

The impacts of N deposition on the accumulation of microbial necromass were also closely associated with soil environment. Clay content has been found to be negatively associated with microbial turnover rates, which was attributed to the limitation of movement and accessibility to resources (Dungait et al., 2012; Wang et al., 2021). Admittedly, a large body of researches has illustrated that microbial necromass forms stable associations with clay minerals, retarding microbial decomposition on necromass (e.g., Miltner et al., 2012; Kallenbach et al., 2016; Liang et al., 2019). However, the enrichment of clay in the soil could also constrain the accessibility of microbial extracellular enzyme to substrate and subsequent microbial growth, limiting the production of microbial necromass (Yang et al., 2020). As a result, microbial necromass contributions to SOC pool was detected to negatively associate with soil clay contents (Fig. 2). In soils with low clay contents, the physical restriction of soil clay particles on microbial growth and metabolism is weak. Accordingly, the inhibition of bacterial necromass accumulation and stimulation of fungal necromass formation under high level of N deposition (Fig. 4a and c) is probably resulted from the susceptible N-induced dominance of fungi in microbial communities (Liang et al., 2016; Shao et al., 2019). Furthermore, soil pH was also an important regulator of microbial turnover (Wang et al., 2021). In general,

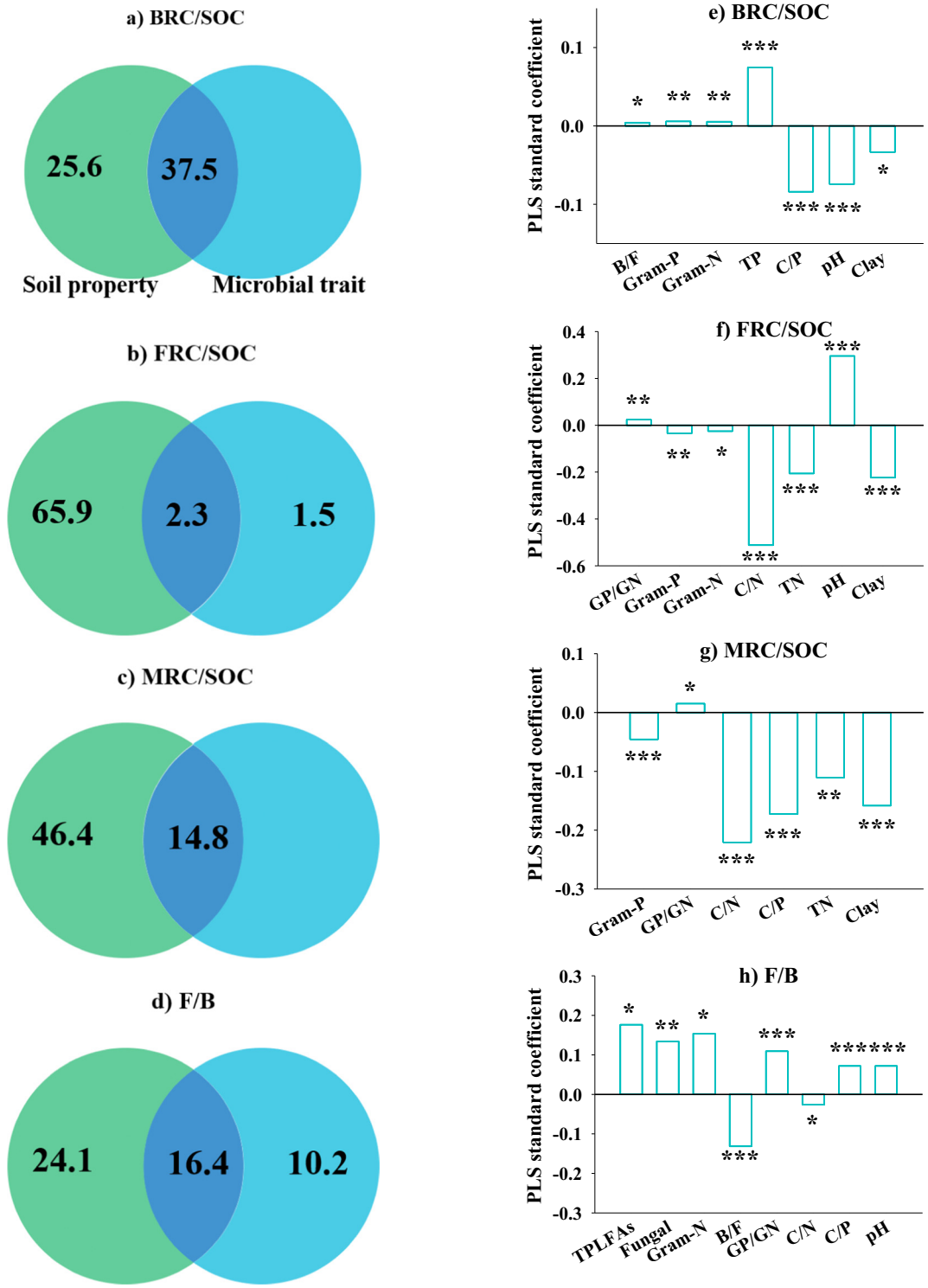

Fig. 3. Variance partitioning for predictors (a-d) and partial least squares (PLS) standardized coefficients of variables (e-h) in determining the contribution of bacterial (a, e), fungal (b, f), the total microbial necromass (c, g) to SOC pool and the ratio of fungal to bacterial necromass (d, h), respectively. Values <0 in variance partitioning analysis are not shown. The PLS coefficient values show the direction and magnitude of the effect of each variable. Variable shown are all significant ($p < 0.05$). MAT and MAP denote the mean annual temperature and the mean annual precipitation, respectively, and GP and GN denote gram-positive and gram-negative bacterial biomass, respectively.

compared to bacteria, fungi predominate in soils with high pH (Thoms and Gleixner, 2013; Zhang et al., 2013). The gradual increase in the dominance of fungi in microbial communities could contribute to the enhanced accumulation of fungal over bacterial residues with increasing pH. Supporting this suggestion, we found that pH correlated negatively with bacterial necromass accumulation whereas positively with fungal necromass accumulation (Fig. 3e and f). Noteworthily, the accumulation of microbial necromass was fiercely differentiated by N deposition in less acidic soils that were generally ascribed to high-latitude forests with N deficiency (Fig. 4b and d). This is probably mediated by the more susceptible responses of bacteria and fungi in N-limited soils following N enrichment (Gutknecht et al., 2012; Wang et al., 2017; Widdig et al., 2020; Moore et al., 2021).

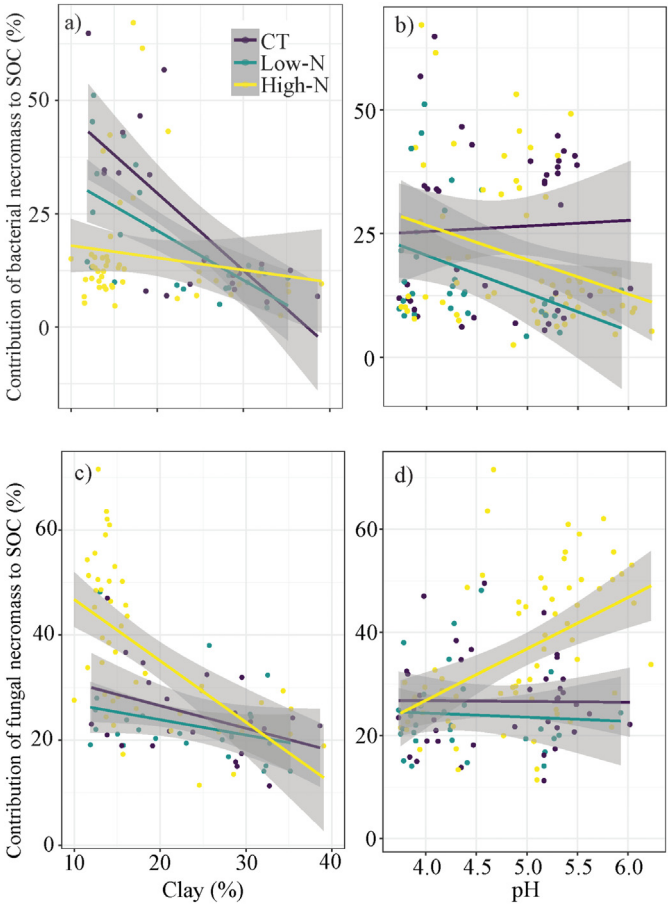

Fig. 4. Relationships between contributions of bacterial (a, b) and fungal necromass to SOC (c-d) and edaphic variables in soils subjected to various N-addition regimes. CT, Low-N, and High-N indicate control (no fertilization, n = 38), low N deposition (≤50 kg N ha^{-1} yr^{-1}, n = 66) and high N deposition (>50 kg N ha^{-1} yr^{-1}, n = 30) treatments, respectively.

Soil properties and microbial community structure conjointly impacted the composition of microbial derived SOC, i.e., the ratio of fungal to bacterial necromass (Fig. 3d). Microbial necromass represent a time-integrated indicator of microbial community growth and biomass turnover, thus the change in the composition of microbial necromass is significantly influenced by the changes in microbial community structure (Liang et al., 2016; Shao et al., 2019). In our study, it can be argued that the changes in the ratio of fungal to bacterial necromass under N deposition might depend on the changes in community structure of soil microorganisms (ratios of bacteria/fungi and gram-positive/gram-negative bacteria) as a result of changes in soil stoichiometric ratio and environmental condition (Ding et al., 2020; Luo et al., 2020).

4.2. N-induced changes in geographical pattern of microbial necromass accumulation

Although apparent impacts of N deposition on the contributions of microbial necromass to SOC were detected, the geographical patterns of the contributions of microbial necromass to SOC pool in control soils without N deposition, as well as their absolute contents, were highly consistent with those in N-treated soils (Fig. 5, S1). This finding confirmed our second hypothesis, and indicated that the geographical patterns might be closely governed by other inherent factors such as climatic factors that derived stronger regulation than N deposition. Climatic factors (i.e., temperature and precipitation) are influential as they are widely demonstrated to regulate microbial processes and function at a large scale (Jing et al., 2020). Furthermore, as affected by the climatic variation along latitudinal gradients, hump-shaped distributions of the contributions of fungal and total microbial necromass to SOC as well as their absolute concentrations with latitude were shaped (Chi et al., 2019; Chen et al., 2020a; Ni et al., 2020a). Low soil temperature in high-latitude biomes restricts microbial activity, allowing the MAT to be a key influencing factor of microbial necromass accumulation (Chen et al., 2020a). In low-latitude acidic forests, however, the high-proton soil shortens the activity period of extracellular enzymes (Rousk et al., 2009; Khan et al., 2016). Therefore, the highest contributions of fungal and total microbial necromass to SOC pool were recorded in mid-latitude regions with favourable soil environments and climatic conditions. In contrast, the linear decrease in the contribution of bacterial necromass to SOC with increasing latitude might be closely governed by MAT and MAP, as both of which positively correlated with the contribution of bacterial necromass to SOC (Fig. 2). In low-latitude forest soils with warmer and wetter environment, the decomposition of plant residues was accelerated to convert by microorganisms, and the turnover of fast-growing bacteria resulted in a relative greater accumulation of bacterial necromass in soils (Chen et al., 2020a; Zhu et al., 2021). Furthermore, the

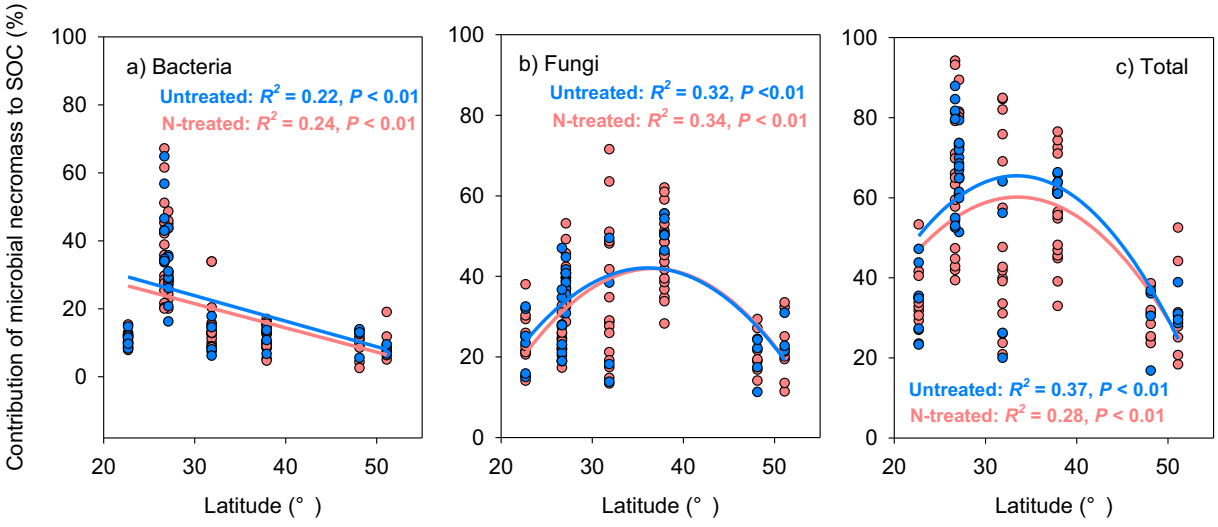

Fig. 5. Latitudinal patterns of the contributions of bacterial (a), fungal (b) and total microbial (c) necromass to SOC pool in N-treated soils (n = 92) and untreated soils (n = 42) across various forest ecosystems.

climatic conditions in low-latitude forests determine that soil parent material is subjected to greater weathering and thus benefit the accumulation of soil P, which is evidenced to positively correlate with the accumulation of soil bacterial necromass (Fan et al., 2020).

4.3. Limitations and implications for future study

Like most current studies that concerned N deposition influence, this study preferentially tested the effect of N amount, but ignored the influence of application frequency. Several studies have shown that the frequency of application can strongly affect soil microbial communities and soil properties (Ning et al., 2015; Wang et al., 2018). Thus, N addition frequency effect might also potentially confound the results. In this study, the 7 different sites suffered N in different amounts and frequencies. However, the limited amount of data in our study might hamper revealing the N frequency effect, increasing the margin of error. Therefore, further studies with abundant samples are called for considering the effect of N addition frequency on soil C dynamics.

5. Conclusion

Overall, we provide evidence for the disproportionate impacts of N deposition on bacterial and fungal necromass accumulation in forest soils in eastern China. The accumulation of fungal necromass got benefited at the expense of bacterial necromass under increased N deposition. Furthermore, distinct geographical patterns of bacterial and fungal necromass contributions to SOC were revealed. Relative to N deposition, the climatic variation along latitudinal gradients exerted much stronger controls on the contributions of bacterial and fungal necromass to SOC at a large scale, leaving the geographical pattern of microbial necromass stable under N deposition. These findings could provide implications for the prediction of the natural distribution of microbial necromass accumulation, in order to enhance the microbial-derived C sequestration in terrestrial ecosystems under global climate change.

Data availability statement

The data that support the findings of this study are available from the corresponding author upon reasonable request.

CRediT authorship contribution statement

This specific study was designed by Q.K.W.; X.Z. and S.L. collected soil samples with assistance from Q.G.W., W.Z. and P.G.; P.T., X.Z., and S.L. conducted the laboratory analysis; P.T. and Q.K.W. analyzed the data and wrote the manuscript with assistance from B.S.R., C.L. and all other co-authors.

Data availability

Data will be made available on request.

Declaration of competing interest

The authors declare that they have no known competing financial interests or personal relationships that could have appeared to influence the work reported in this paper.

Acknowledgment

This work was supported by the National Natural Science Foundation of China (grant no. 31830015, 32171752, 32101334). We also thanks Yifan Zhu, Jing Li and Lei Yang for their helps when analyzing soil microbial necromass and PLFAs. We are very thankful to the editor and reviewers for their constructive comments and valuable suggestions on an earlier version of this manuscript.

Appendix A. Supplementary data

Supplementary data to this article can be found online at https://doi.org/10.1016/j.scitotenv.2022.157645.

References

Appuhn, A., Joergensen, R.G., 2006. Microbial colonisation of roots as a function of plant species. Soil Biol. Biochem. 38 (5), 1040–1051. https://doi.org/10.1016/j.soilb io.2005.09.002.
Chen, G., Ma, S., Tian, D., Xiao, W., Jiang, L., Xing, A., Zou, A., Zhou, L., Shen, H., Zheng, C., Ji, C., He, H., Zhu, B., Liu, L., Fang, J., 2020a. Patterns and determinants of soil microbial residues from tropical to boreal forests. Soil Biol. Biochem. 151, 108059. https://doi.org/10.1016/j.soilbio.2020.108059.
Chen, J., Xiao, W., Zheng, C., Zhu, B., 2020b. Nitrogen addition has contrasting effects on particulate and mineral-associated soil organic carbon in a subtropical forest. Soil Biol. Biochem. 142, 107708. https://doi.org/10.1016/j.soilbio.2020.107708.
Chi, J., Zhang, W., Wang, L., Putnis, C., 2019. Direct observations of the occlusion of soil organic matter within calcite. Environ. Sci. Technol. 53 (14), 8097–8104. https://doi.org/10.1021/acs.est.8b06807.
Cotrufo, M.F., Soong, J.L., Horton, A.J., Campbell, E.E., Haddix, M.L., Wall, D.H., Parton, W.J., 2015. Formation of soil organic matter via biochemical and physical pathways of litter mass loss. Nat. Geosci. 8 (10), 776–779. https://doi.org/10.1038/NGEO2520.
Cyle, K.T., Hill, N., Young, K., Jenkins, T., Hancock, D., Schroeder, P.A., 2016. Substrate quality influences organic matter accumulation in the soil silt and clay fraction. Soil Biol. Biochem. 103, 138–148. https://doi.org/10.1016/j.soilbio.2016.08.014.
Ding, X.L., Chen, S.Y., Zhang, B., He, H.B., Filley, T.R., Horwath, W.R., 2020. Warming yields distinct accumulation patterns of microbial residues in dry and wet alpine grasslands on the Qinghai-Tibetan plateau. Biol. Fert. Soils 56, 881–892. https://doi.org/10.1007/s00374-020-01474-9.
Du, E., Terrer, C., Pellegrini, A.F.A., Ahlström, A., van Lissa, C.J., Zhao, X., Xia, N., Wu, X., Jackson, R.B., 2020. Global patterns of terrestrial nitrogen and phosphorus limitation. Nat. Geosci. 13, 221–226. https://doi.org/10.1038/s41561-019-0530-4.
Dungait, J.A.J., Hopkins, D.W., Gregory, A.S., Whitmore, A.P., 2012. Soil organic matter turnover is governed by accessibility not recalcitrance. Glob. Chang. Biol. 18 (6), 1781–1796. https://doi.org/10.1111/j.1365-2486.2012.02665.x.
Eastman, B.A., Adams, M.B., Peterjohn, W.T., 2022. The path less taken: long-term N additions slow leaf litter decomposition and favor the physical transfer pathway of soil organic matter formation. Soil Biol. Biochem. 166, 108567. https://doi.org/10.1016/j.soilbio.2022.108567.
Fan, Y.X., Yang, L.M., Zhong, X.J., Yang, Z.J., Lin, Y.Y., Guo, J.F., Chen, G.S., Yang, Y.S., 2020. N addition increased microbial residual carbon by altering soil P availability and microbial composition in a subtropical castanopsis forest. Geoderma 375, 114470. https://doi.org/10.1016/j.geoderma.2020.114470.
Geyer, K.M., Kyker-Snowman, E., Grandy, A.S., Frey, S.D., 2016. Microbial carbon use efficiency: accounting for population, community, and ecosystem-scale controls over the fate of metabolized organic matter. Biogeochemistry 127, 173–188. https://doi.org/10.1007/s10533-016-0191-y.
Griepentrog, M., Bode, S., Boeckx, P., Hagedorn, F., Heim, A.R., Schmidt, M.W.I., 2014. Nitrogen deposition promotes the production of new fungal residues but retards the decomposition of old residues in forest soil fractions. Glob. Chang. Biol. 20 (1), 327–340. https://doi.org/10.1111/gcb.12374.
Gutknecht, J.L.M., Field, C.B., Balser, T.C., 2012. Microbial communities and their responses to simulated global change fluctuate greatly over multiple years. Glob. Chang. Biol. 18 (7), 2256–2269. https://doi.org/10.1111/j.1365-2486.2012.02686.x.
Janssens, I.A., Dieleman, W., Luyssaert, S., Subke, J.A., Reichstein, M., Ceulemans, R., Ciais, P., Dolman, A.J., Grace, J., Matteucci, G., Papale, D., Piao, S.L., Schulze, E.D., Tang, J., Law, B.E., 2010. Reduction of forest soil respiration in response to nitrogen deposition. Nat. Geosci. 3, 315. https://doi.org/10.1038/NGEO844.
Jing, X., Chen, X., Fang, J.Y., Ji, C.J., Shen, H.H., Zheng, C.Y., Zhu, B., 2020. Soil microbial carbon and nutrient constraints are driven more by climate and soil physicochemical properties than by nutrient addition in forest ecosystems. Soil Biol. Biochem. 141, 107657. https://doi.org/10.1016/j.soilbio.2019.107657.
Jones, D.L., Hill, P.W., Smith, A.R., Farrell, M., Ge, T., Banning, N.C., Murphy, D.V., 2018. Role of substrate supply on microbial carbon use efficiency and its role in interpreting soil microbial community-level physiological profile (CLPP). Soil Biol. Biochem. 123, 1–6. https://doi.org/10.1016/j.soilb io.2018.04.014.
Kaiser, C., Koranda, M., Kitzler, B., Fuchslueger, L., Schnecker, J., Schweiger, P., Rasche, F., Zechmeister-Boltenstern, S., Sessitsch, A., Richter, A., 2010. Belowground carbon allocation by trees drives seasonal patterns of extracellular enzyme activities by altering microbial community composition in a beech forest soil. New Phytol. 187 (3), 843–858. https://doi.org/10.1111/j.1469-8137.2010.03321.x.
Kallenbach, C.M., Frey, S.D., Grandy, A.S., 2016. Direct evidence for microbial-derived soil organic matter formation and its ecophysiological controls. Nat. Commun. 7, 13630. https://doi.org/10.1038/ncomms13630.
Kästner, M., Miltner, A., 2018. Chapter 5 - SOM and microbes—what is left from microbial life. In: Nannipieri, P., Hernandez, T. (Eds.), The Future of Soil Carbon. Academic Press, pp. 125–163.
Khan, K.S., Mack, R., Castillo, X., Kaiser, M., Joergensen, R.G., 2016. Microbial biomass, fungal and bacterial residues, and their relationships to the soil organic matter C/N/P/S ratios. Geoderma 271, 115–123. https://doi.org/10.1016/j.geoderma.2016.02.019.
Lal, R., 2008. Carbon sequestration. Phil. Trans. R. Soc. B. 363, 815–830. https://doi.org/10.1098/rstb.2007.2185.
Lehmann, J., Kleber, M., 2015. The contentious nature of soil organic matter. Nature 528, 60–68. https://doi.org/10.1038/natur e16069.

Liang, C., Amelung, W., Lehmann, J., Kästner, M., 2019. Quantitative assessment of microbial necromass contribution to soil organic matter. Glob. Chang. Biol. 25 (11), 3578–3590. https://doi.org/10.1111/gcb.14781.

Liang, C., Balser, T.C., 2011. Microbial production of recalcitrant organic matter in global soils: implications for productivity and climate policy. Nat. Rev. Microbiol. 9 (1), 75. https://doi.org/10.1038/nrmicro2386-c1.

Liang, C., Balser, T.C., 2012. Warming and nitrogen deposition lessen microbial residue contribution to soil carbon pool. Nat. Commun. 3, 1222. https://doi.org/10.1038/ncomms2224.

Liang, C., Kao-Kniffin, J., Sanford, G.R., Wickings, K., Balser, T.C., Jackson, R.D., 2016. Microorganisms and their residues under restored perennial grassland communities of varying diversity. Soil Biol. Biochem. 103, 192–200. https://doi.org/10.1016/j.soilbio.2016.08.002.

Liang, C., Schimel, J.D., Jastrow, J.D., 2017. The importance of anabolism in microbial control over soil carbon storage. Nat. Microbiol. 2, 17105. https://doi.org/10.1038/nmicrobiol.2017.105.

Ludwig, M., Achtenhagen, J., Miltner, A., Eckhardt, K.-U., Leinweber, P., Emmerling, C., Thiele-Bruhn, S., 2015. Microbial contribution to SOM quantity and quality in density fractions of temperate arable soils. Soil Biol. Biochem. 81, 311–322. https://doi.org/10.1016/j.soilbio.2014.12.002.

Luo, R.Y., Kuzyakov, Y., Liu, D.Y., Fan, J.L., Luo, J.F., Lindsey, S., He, J.S., Ding, W.X., 2020. Nutrient addition reduces carbon sequestration in a tibetan grassland soil: disentangling microbial and physical controls. Soil Biol. Biochem. 144, 107764. https://doi.org/10.1016/j.soilbio.2020.107764.

Lu, R.K., 2000. Methods of Soil Agricultural Chemistry Analysis. Chinese Agricultural Science and Technology Press, Beijing, pp. 24–26.

Lu, X., Hou, E., Guo, J., Gilliam, F.S., Li, J., Tang, S., Kuang, Y., 2021a. Nitrogen addition stimulates soil aggregation and enhances carbon storage in terrestrial ecosystems of China: a meta-analysis. Glob. Chang. Biol. 27, 2780–2792. https://doi.org/10.1111/gcb.15604.

Lu, X., Vitousek, P.M., Mao, Q., Gilliam, F.S., Luo, Y., Turner, B.L., Zhou, G., Mo, J., 2021b. Nitrogen deposition accelerates soil carbon sequestration in tropical forests. Proc. Natl. Acad. Sci. U. S. A. 118, e2020790118. https://doi.org/10.1073/pnas.2020790118.

Ma, S.H., Chen, G.P., Tian, D., Du, E.Z., Xiao, W., Jiang, L., Zhou, Z., Zhu, J.L., He, H.B., Zhu, B., Fang, J.Y., 2020. Effects of seven-year nitrogen and phosphorus additions on soil microbial community structures and residues in a tropical forest in Hainan Island. China. Geoderma 361, 114034. https://doi.org/10.1016/j.geoderma.2019.114034.

Ma, T., Zhu, S.S., Wang, Z.H., Chen, D.M., Dai, G.H., Feng, B.W., Su, X.Y., Hu, H.F., Li, K.H., Han, W.X., Liang, C., Bai, Y.F., Feng, X.J., 2018. Divergent accumulation of microbial necromass and plant lignin components in grassland soils. Nat. Commun. 9 (1), 3480. https://doi.org/10.1038/s41467-018-05891-1.

Miltner, A., Bombach, P., Schmidt-Brücken, B., Kästner, M., 2012. SOM genesis: microbial biomass as a significant source. Biogeochemistry 111, 41–55. https://doi.org/10.1007/s10533-011-9658-z.

Moore, J.A.M., Anthony, M.A., Pec, G.J., Trocha, L.K., Trzebny, A., Geyer, K.M., van Diepen, L.T.A., Frey, S.D., 2021. Fungal community structure and function shifts with atmospheric nitrogen deposition. Glob. Chang. Biol. 27 (7), 1349–1364. https://doi.org/10.1111/gcb.15444.

Ni, H.W., Jing, X.Y., Xiao, X., Zhang, N., Wang, X.Y., Sui, Y.Y., Sun, B., Liang, Y.T., 2021. Microbial metabolism and necromass mediated fertilization effect on soil organic carbon after long-term community incubation in different climates. ISME J. 15 (9), 2561–2573. https://doi.org/10.1038/s41396-021-00950-w.

Ni, X.Y., Liao, S., Tan, S.Y., Wang, D.Y., Peng, Y., Yue, K., Wu, F.Z., Yang, Y.S., 2020a. A quantitative assessment of amino sugars in soil profiles. Soil Biol. Biochem. 143, 107762. https://doi.org/10.1016/j.soilbio.2020.107762.

Ni, X.Y., Liao, S., Tan, S.Y., Peng, Y., Wang, D.Y., Yue, K., Wu, F.Z., Yang, Y.S., Xu, X.F., 2020b. The vertical distribution and control of microbial necromass carbon in forest soils. Glob. Ecol. Biogeogr. 29 (10), 1829–1839. https://doi.org/10.1111/geb.13159.

Ning, Q., Gu, Q., Shen, J., Lv, X., Yang, J., Zhang, X., He, J., Huang, J., Wang, H., Xu, Z., Han, X., 2015. Effects of nitrogen deposition rates and frequencies on the abundance of soil nitrogen-related functional genes in temperate grassland of northern China. J. Soils Sediments 15 (3), 694–704. https://doi.org/10.1007/s11368-015-1061-2.

R Development Core Team, 2020. R: A language and environment for statistical computing. R Foundation for Statistical Computing. https://www.R-project.org.

Rinnan, R., Bååth, E., 2009. Differential utilization of carbon substrates by bacteria and fungi in tundra soil. Appl. Environ. Microb. 75 (11), 3611–3620. https://doi.org/10.1128/aem.02865-08.

Rousk, J., Brookes, P.C., Bååth, E., 2009. Contrasting soil pH effects on fungal and bacterial growth suggest functional redundancy in carbon mineralization. Appl. Environ. Microb. 75 (6), 1589–1596. https://doi.org/10.1128/AEM.02775-08.

Sanchez, G., 2013. PLS path modeling with R. Trowchez Editions. http://creativecommons.org/licenses/by-nc-sa/3.0/.

Schmidt, M.W.I., Torn, M.S., Abiven, S., Dittmar, T., Guggenberger, G., Janssens, I.A., Kleber, M., Kogel-Knabner, I., Lehmann, J., Manning, D.A.C., Nannipieri, P., Rasse, D.P., Weiner, S., Trumbore, S.E., 2011. Persistence of soil organic matter as an ecosystem property. Nature 478 (7367), 49–56. https://doi.org/10.1038/natur e10386.

Schulte-Uebbing, L., de Vries, W., 2018. Global-scale impacts of nitrogen deposition on tree carbon sequestration in tropical, temperate, and boreal forests: A meta-analysis. Glob. Chang. Biol. 24 (2), e416–e431. https://doi.org/10.1111/gcb.13862.

Shao, P., Liang, C., Lynch, L., Xie, H., Bao, X., 2019. Reforestation accelerates soil organic carbon accumulation: evidence from microbial biomarkers. Soil Biol. Biochem. 131, 182–190. https://doi.org/10.1016/j.soilbio.2019.01.012.

Thomas, R.Q., Canham, C.D., Weathers, K.C., Goodale, C.L., 2010. Increased tree carbon storage in response to nitrogen deposition in the US. Nat. Geosci. 3, 13–17. https://doi.org/10.1038/ngeo721.

Thoms, C., Gleixner, G., 2013. Seasonal differences in tree species' influence on soil microbial communities. Soil Biol. Biochem. 66, 239–248. https://doi.org/10.1016/j.soilbio.2013.05.018.

Wang, C., Qu, L., Yang, L., Liu, D., Morrissey, E., Miao, R., Liu, Z., Wang, Q., Fang, Y., Bai, E., 2021. Large-scale importance of microbial carbon use efficiency and necromass to soil organic carbon. Glob. Chang. Biol. 27 (10), 2039–2048. https://doi.org/10.1111/gcb.15550.

Wang, Q.K., Zhang, W.D., Sun, T., Chen, L.C., Pang, X.Y., Wang, Y.P., Xiao, F.M., 2017. N and P fertilization reduced soil autotrophic and heterotrophic respiration in a young Cunninghamia lanceolata forest. Agric. For. Meteorol. 232, 66–73. https://doi.org/10.1016/j.agrformet.2016.08.007.

Wang, R., Zhang, Y., He, P., Yin, J., Yang, J., Liu, H., Cai, J., Shi, Z., Feng, X., Dijkstra, F.A., Han, X., Jiang, Y., 2018. Intensity and frequency of nitrogen addition alter soil chemical properties depending on mowing management in a temperate steppe. J. Environ. Manag. 224, 77–86. https://doi.org/10.1016/j.jenvman.2018.07.036.

White, D.C., Ringelberg, D.B., 1998. Signature lipid biomarker analysis. In: Burlage, R.S., Atlas, R., Stahl, D., Geesey, G., Sayler, G. (Eds.), Techniques in Microbial Ecology. Oxford University Press, New York, pp. 255–272.

Widdig, M., Heintz-Buschart, A., Schleuss, P.-M., Guhr, A., Borer, E.T., Seabloom, E.W., Spohn, M., 2020. Effects of nitrogen and phosphorus addition on microbial community composition and element cycling in a grassland soil. Soil Biol. Biochem. 151, 108041. https://doi.org/10.1016/j.soilbio.2020.108041.

Wilpiszeski, R.L., Aufrecht, J.A., Retterer, S.T., Sullivan, M.B., Graham, D.E., Pierce, E.M., Zablocki, O.D., Palumbo, A.V., Elias, D.A., 2019. Soil aggregate microbial communities: towards understanding microbiome interactions at biologically relevant scales. Appl. Environ. Microb. 85 (14), e00324-19. https://doi.org/10.1128/AEM.00324-19.

Yang, L., Lyu, M., Li, X., Xiong, X., Lin, W., Yang, Y., Xie, J., 2020. Decline in the contribution of microbial residues to soil organic carbon along a subtropical elevation gradient. Sci. Total Environ. 749, 141583. https://doi.org/10.1016/j.scitotenv.2020.141583.

Zhang, B., Liang, C., He, H., Zhang, X., 2013. Variations in soil microbial communities and residues along an altitude gradient on the northern slope of Changbai mountain, China. PLoS One 8, e66184. https://doi.org/10.1371/journal.pone.0066184.

Zhang, W., Cui, Y.H., Lu, X.K., Bai, E., He, H.B., Xie, H.T., Liang, C., Zhang, X.D., 2016. High nitrogen deposition decreases the contribution of fungal residues to soil carbon pools in a tropical forest ecosystem. Soil Biol. Biochem. 97, 211–214. https://doi.org/10.1016/j.soilbio.2016.03.019.

Zhang, X.D., Amelung, W., 1996. Gas chromatographic determination of muramic acid, glucosamine, mannosamine, and galactosamine in soils. Soil Biol. Biochem. 28, 1201–1206. https://doi.org/10.1016/0038-0717(96)00117-4.

Zhu, E., Cao, Z., Jia, J., Liu, C., Zhang, Z., Wang, H., Dai, G., He, J.S., Feng, X., 2021. Inactive and inefficient: warming and drought effect on microbial carbon processing in alpine grassland at depth. Glob. Chang. Biol. 27 (10), 2241–2253. https://doi.org/10.1111/gcb.15541.